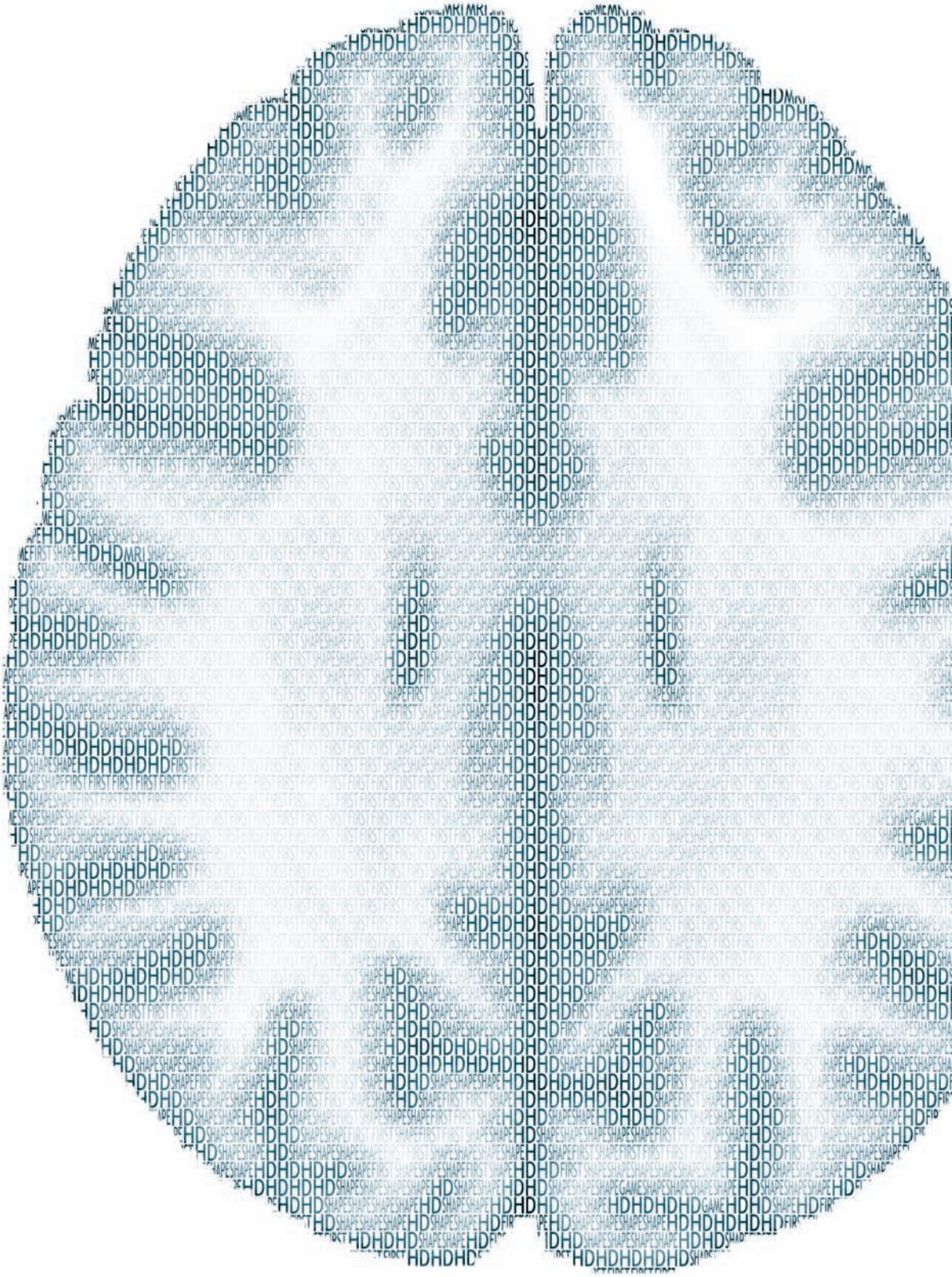

Chapter 4

Shape analysis of subcortical nuclei in Huntington's disease, global versus local atrophy - Results from the TRACK-HD study

Simon J.A. van den Bogaard[1], Eve M. Dumas[1], Luca Ferrarini[2], Julien Milles[2], Mark A. van Buchem[3], Jeroen van der Grond[3], Raymund A.C. Roos[1]

1. Department of Neurology, Leiden University Medical Center, Leiden, the Netherlands
2. Division of Image Processing (LKEB), Department of Radiology, Leiden University Medical Center, Leiden, the Netherlands
3.Department of Radiology, Leiden University Medical Center, Leiden, the Netherlands

Journal of the Neurological Sciences (2011) 307:60-68

Abstract

Huntington's disease (HD) is characterized by brain atrophy. Localized atrophy of a specific structure could potentially be a more sensitive biomarker reflecting neuropathologic changes rather than global volume variation. We examined 90 TRACK-HD participants of which 30 were premanifest HD, 30 were manifest HD and 30 were controls. Using FMRIB's Integrated Registration and Segmentation Tool, segmentations were obtained for the pallidum, caudate nucleus, putamen, thalamus, accumbens nucleus, amygdala, and hippocampus and overall volumes were calculated. A point distribution model of each structure was obtained using Growing and Adaptive Meshes. Permutation testing between groups was performed to detect local displacement in shape between groups. In premanifest HD overall volume loss occurred in the putamen, accumbens and caudate nucleus. Overall volume reductions in manifest HD were found in all subcortical structures, except the amygdala, as compared to controls. In premanifest HD shape analysis showed small areas of displacement in the putamen, pallidum, accumbens and caudate nucleus. When the premanifest group was split into two groups according to predicted disease onset, the premanifest HD group close to expected disease onset showed more pronounced displacements in caudate nucleus and putamen compared to premanifest HD far from disease onset or the total premanifest group. Analysis of shape in manifest HD showed widespread shape differences, most prominently in the caudal part of the accumbens nucleus, body of the caudate nucleus, putamen and dorsal part of the pallidum. We conclude that shape analysis provides new insights in localized intrastructural atrophy patterns in HD, but can also potentially serve as specific target areas for disease tracking.

Introduction

Huntington's disease (HD) is a slowly progressive neurodegenerative genetic disease that affects the brain. Disease onset occurs typically between the age of 35 and 45 years, with clinical symptoms in motor, cognitive and behavior domains. Since the discovery of the genetic defect on chromosome 4, the gene status of at-risk individuals can be determined, making identification of premanifest gene carriers possible. This makes examination of brain structures possible in this symptom free period, and can provide insight into pathophysiological changes underlying the disease.

Currently, many studies focus on finding reliable markers to monitor disease progression[1;2]. MRI measures show great potential of becoming sensitive biomarkers for HD, as they are objective and have been applied to demonstrate abnormalities of both gray and white matter structures[3]. Changes in basal ganglia are of special interest as these structures display overall volume reduction in the premanifest stages of HD. The caudate nucleus and putamen are reported to be atrophied up to a decade before disease onset[1;2;4].

Two pathologic studies report on localized loss of neurons within a structure, namely within the medial paraventricular portions of the caudate nucleus, in the tail of the caudate nucleus, and in the dorsal part of the putamen in a dorsal ventral manner[5;6]. Currently, in vivo measures of atrophy have predominantly reported overall volumetric change of a structure, representing a generalized loss of neurons and axons. Unrepresented in this approach is localized loss of neurons, or any other remodeling effects, which go unnoticed if these local changes do not significantly affect the total volume of the structure.

To examine how subcortical nuclei change locally, we have chosen an automated MRI analysis set-up using FMRIB's Integrated Registration and Segmentation Tool (FIRST) and the Growing and Adaptive Meshes (GAMEs) tools. This approach is chosen because in this way we obtain a per participant individual segmentation and outer surface of several subcortical structures. This approach is fundamentally different from Voxel Based Morphometry (VBM) where a voxel wise comparison is made between groups, also in this way we avoid some known methodological issues associated with VBM[7;8].

The TRACK-HD study is a biomarker study[1], dedicated to finding objective and sensitive measures for disease progression. This study allows examination of a

well defined cohort of premanifest gene carriers, manifest HD and controls. The aim of our study is to determine how the subcortical nuclei locally change in shape in the premanifest and the manifest stage of HD in relation to global volumetric changes.

Methods

Subjects

The multicentre Track-HD cohort consists in total of 366 participants. All of the 90 participants enrolled at the Leiden University Medical Centre from the TRACK-HD cohort were included for this analysis (premanifest HD n=30, manifest HD n=30, control n=30). Inclusion criteria for the premanifest group consisted of a CAG repeat length ≥ 40, absence of motor disturbances on the Unified Huntington's Disease Rating Scale (UHDRS) defined as a total motor score (TMS) ≤ 5. The UHDRS TMS is a clinical rating of the amount of motor disturbances, grading several distinct motor features separately such as chorea, dystonia, rigidity, bradykinesia and eye movements, resulting in a sum score ranging from 0 to124. Additionally a disease burden score of ≥ 250 was mandatory to ensure that the premanifest group was within 16 years of the predicted age of onset[9;10]. For an additional analysis within the premanifest group, a further subdivision of the group was performed on the basis of the median predicted years to diagnosis into premanifest A (10.8 or more years to disease onset, N = 16) and premanifest B (closer than 10.8 years to disease onset, N = 14) based on Langbehn's *et al.* (2004, 2010) survival analysis formula[10;11] identical to previous reports from the TRACK-HD study[1;12]. Inclusion criteria for the manifest HD group consisted of a CAG repeat ≥ 40, a TMS > 5 and a Total Functional Capacity (TFC) ≥ 7. The TFC is a clinical scale assessing the activities in daily life (range 0-13) such as job capability, finances, daily chores and self care. Healthy gene negative family members or partners/spouses were included as controls. Exclusion criteria consisted of any significant (neurological) comorbidity, history of severe head trauma, a major psychiatric diagnosis and MRI incompatibility. The medical ethical committee approved the study, and written informed consent was obtained from all participants. Detailed description of recruitment and inclusion criteria is given in the TRACK-HD baseline paper[1].

MRI acquisition

In accordance with the TRACK-HD protocol, all participants underwent MRI scanning on a 3 Tesla Philips whole body scanner (Philips Medical Systems, Best, The Netherlands) with an eight channel receive and transmit coil array. T1-

weighted image volumes were acquired using a 3D MPRAGE acquisition sequence with the following imaging parameters: TR = 7.7ms, TE= 3.5ms, FA= 8°, FOV= 24cm, matrix size 224x224x164 with sagittal slices to cover the entire brain with a slice thickness of 1.0 mm with no gap between slices, total acquisition time was ~9 minutes.

Post-Processing and Statistics

The analysis pipeline is depicted in figure 1.

Analysis processing pipeline

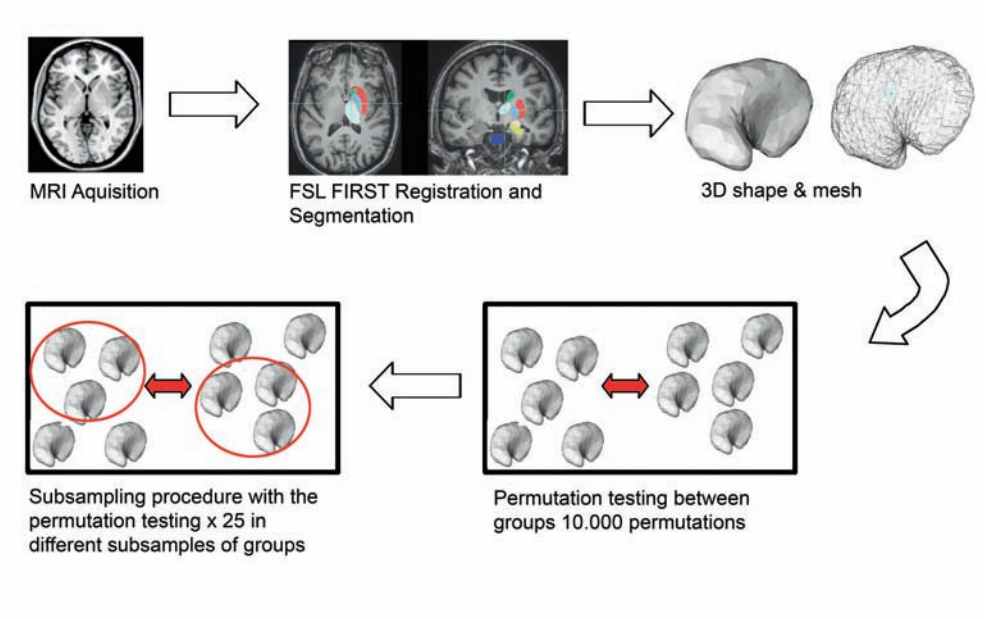

Figure 1: Analysis processing pipeline from MRI acquisition to Hotelling's T2 statistics

Overall volume analysis

Using FMRIB's Integrated Registration and Segmentation Tool (FIRST), subcortical nuclei were affine registered to MNI152 standard space using linear registration and subsequently automatically segmented[13;14]. Volumes for pallidum, caudate nucleus, putamen, thalamus, accumbens nucleus, amygdala, and the hippocampus were calculated. Analysis of variance was performed, correcting for age, gender and intracranial volume (ICV).

The rationale to use FSL FIRST as our registration and segmentation tool was the fact that the tool has an automated set-up and is therefore an unbiased approach.

The validity of the tool to register and segment with great accuracy is described by Patenaude *et al.* (2007, 2008)[13-15]. Furthermore the automated set-up makes it relatively easy to use in large cohorts. A previous study showed the reliable use of this tool in HD for volumetric analysis in HD[12]. This tool has been and is currently being used in many other studies regarding different neurological disorders, among others in Alzheimer's Disease[16]. FSL FIRST has been compared to another automated segmentation tool, namely Freesurfer, with comparison to manual segmentation. It was concluded that Freesurfer provided better results for the hippocampus and FIRST for the amygdala in terms of segmentation and shape analysis. However, also relevant is the comparison they made to expert manual segmentation, where no significant difference was found for the amygdala volume manual versus FIRST segmentation[17]. FIRST performed better in the smaller subcortical structures in a scan-rescan study[18], and since TRACK-HD is set-up as a longitudinal study this is the logical choice considering all of the above arguments. However, it must be noted that all these methodological studies make use of a healthy control group, and to our knowledge no study comparing expert manual tracing versus automated segmentation in diseased/atrophied states exists.

Additional quality control was performed via a visual inspection of all the segmentations using the original T1-weighted scans and projecting the individual segmentations on top of these images. Special attention was given to the outliers in terms of volume. Several registration errors resulted in erroneous segmentations and subsequently these scans were re-run until satisfactory segmentations were acquired. No significant mismatches were visually seen after these steps.

Shape Analysis

To perform shape analysis, comparative meshes for each structure were built. For this purpose the Growing and Adaptive Meshes (GAMEs) algorithm was utilized[19], making use of the segmentations acquired from FIRST. GAMEs has been previously successfully applied for analyzing shape variations in Alzheimer's disease[20;21]. This algorithm builds a deformable surface mesh model based on an average of the 30 control group segmentations. This general mesh model consists of numerous nodes which are equal in number for all meshes used for the comparative analysis across groups. Using these meshes, local shape analysis was performed by repeated permutation tests via a Hotelling's T2 statistical test. The following procedure was applied: a subsampling process was performed, with random samples taken from the control and the HD group; subsequently, permutation test (based on 10.000 iterations, in order to allow for *p*-values as low as 10^{-4}) were performed to detect significant different location between groups, at a

confidence level of 99%. In total 25 sub-sampling iterations were performed, each sub-sample containing a minimum of 60% of the entire group population. For each node the significance level was assessed for all structures analyzed. The latter step is to ensure that the findings are not due to outliers in either the control or the HD group. True findings appear in the majority of the subsample analyses, which can be defined as either 80 or 95% of the subsamples depending on the desired statistical scrutiny. Graphical display does not only show the area of the surface affected in 80-95% of the sub-sampling, but also the amount of displacement in millimeters. We have chosen to use the most conservative option, namely the 95% level; thus the significant locations are at an $\alpha=0.01$, 95% of the times in which the sub-sampling was performed. Three groups were included in the analysis, and the comparisons are displayed for the premanifest group versus the control group and secondly the manifest HD group versus the control group. An additional analysis was performed in an identical manner with the premanifest A and premanifest B groups both compared to the control group. The rationale to perform this additional analysis lies in the fact that there were only limited findings in the premanifest group, which could be due to the fact of a heterogenous premanifest group in terms of predicted years to disease onset. This was addressed by the subdivision of the premanifest group according to predicted disease onset as described above; however noted was the potential disadvantage of loss of statistical power.

Results

Demographic characteristics of the study groups

The clinical features of the three groups are shown in table 1. There were no statistically significant differences between the control and premanifest group. The UHDRS total motor score and total functional capacity were different between the manifest and control or premanifest group.

Table 1: Group characteristics

	Control (Mean ± SD)	Premanifest HD (Mean ± SD)	Manifest HD (Mean ± SD)
Age	48.6 ± 8.3	43.3 ± 8.0	47.6 ± 10.3
CAG	n.e.	42.5 ± 2.4	43.6 ± 2.6
Years to onset	n.a.	11.6 ± 4.3	n.a.
UHDRS TMS	2.6 ± 2.4	2.5 ± 1.4	21.9 ± 11.1 *
TFC	13.0 ± 0.2	12.6 ± 0.8	10.4 ± 2.0 *
Gender (N ♀/♂)	16/14	18/12	21/9

Demographic variables of the three groups. CAG = Cytosine-Adenosine-Guanine repeat. UHDRS = Unified Huntington's Disease Rating Scale Total Motor Score, TFC = Total Functional Capacity. n.a. = not applicable, n.e = not examined.* = significant different from the control and premanifest HD group with $p < 0.05$.

Volumetric analysis

Significant differences in overall volumes between the premanifest and control group were apparent in the accumbens nucleus, caudate nucleus, left hippocampus and putamen. In the manifest HD group all volumes were significantly reduced as compared to controls, except for the amygdala. The overall volumes are shown in table 2.

Shape analysis

The shape analyses for the basal ganglia structures accumbens nucleus, caudate nucleus, pallidum and putamen are displayed in figure 2. The remaining structures amygdala, hippocampus and thalamus are shown in figure 3. The displacements shown in the figures are all significant at the 99% significance level, with the colour coding of the amount of displacements in millimeters. All displacements were inwards, representing atrophy. No significant areas of hypertrophy were observed.

For the accumbens nucleus it is apparent that the shape changes were localized at the caudal side, most prominently seen in the manifest stage. In the premanifest stage a displacement is seen in the right accumbens nucleus. The caudate nucleus showed displacements in both the premanifest and manifest HD groups. A generalized displacement is seen across the whole caudate nucleus, most significantly in the body on the medial side. In premanifest HD significant displacement is seen in some areas more towards the tail. The pallidum showed a diffuse pattern of displacement in the manifest HD group, with the dorsal part displaying the most extensive displacements. Displacement is also seen in this

part of the dorsal pallidum in the premanifest HD group. The putamen showed displacement over the entire structure in the manifest stage, small patches were found in the premanifest stage on the medial side of the left putamen.

For the amygdala the shape changes were seen in the manifest stage, specifically on the cranial side. No displacements were seen in the premanifest group. The hippocampus showed patchy displacement areas at the ventral as well as the dorsal part, this displacement being limited to the manifest group only. Finally the thalamus showed some patchy displacements on the ventro-medial and ventro-lateral side of the structure, but no real displacement areas could be found in the premanifest group.

Table 2: Volumes of subcortical nuclei

	Control		Premanifest HD		Manifest HD	
	Mean volume	SD	Mean Volume	SD	Mean Volume	SD
Accumbens Nucleus						
Right	0.444	0.135	0.369 *	0.107	0.356 *	0.184
Left	0.605	0.136	0.544 *	0.112	0.381 **	0.140
Amygdala						
Right	1.344	0.191	1.376	0.312	1.251	0.307
Left	1.216	0.316	1.218	0.381	1.084	0.343
Caudate Nucleus						
Right	3.339	0.504	2.922 *	0.430	2.450 **	0.447
Left	3.207	0.399	2.848 *	0.493	2.283 **	0.394
Hippocampus						
Right	3.855	0.658	3.820	0.664	3.132 **	0.671
Left	3.660	0.570	3.390 *	0.510	3.121 **	0.478
Pallidum						
Right	1.528	0.278	1.443	0.326	1.025 **	0.319
Left	1.648	0.348	1.524	0.331	1.071 **	0.333
Putamen						
Right	4.597	0.692	4.078 *	0.690	3.283 **	0.463
Left	4.664	0.742	4.176 *	0.607	3.255 **	0.511
Thalamus						
Right	7.424	0.605	7.432	0.730	6.795 *	0.806
Left	7.328	0.840	7.260	0.894	6.782 *	0.794

Volumetric analysis of seven structures. Means are the absolute measured values (mm^3). Significance is after correction for intracranial

volume, gender and age

* significant difference from controls $p < 0.05$

** significant difference from controls $p < 0.001$

Shape analysis of accumbens nucleus, caudate nucleus, pallidum and putamen in premanifest and manifest HD

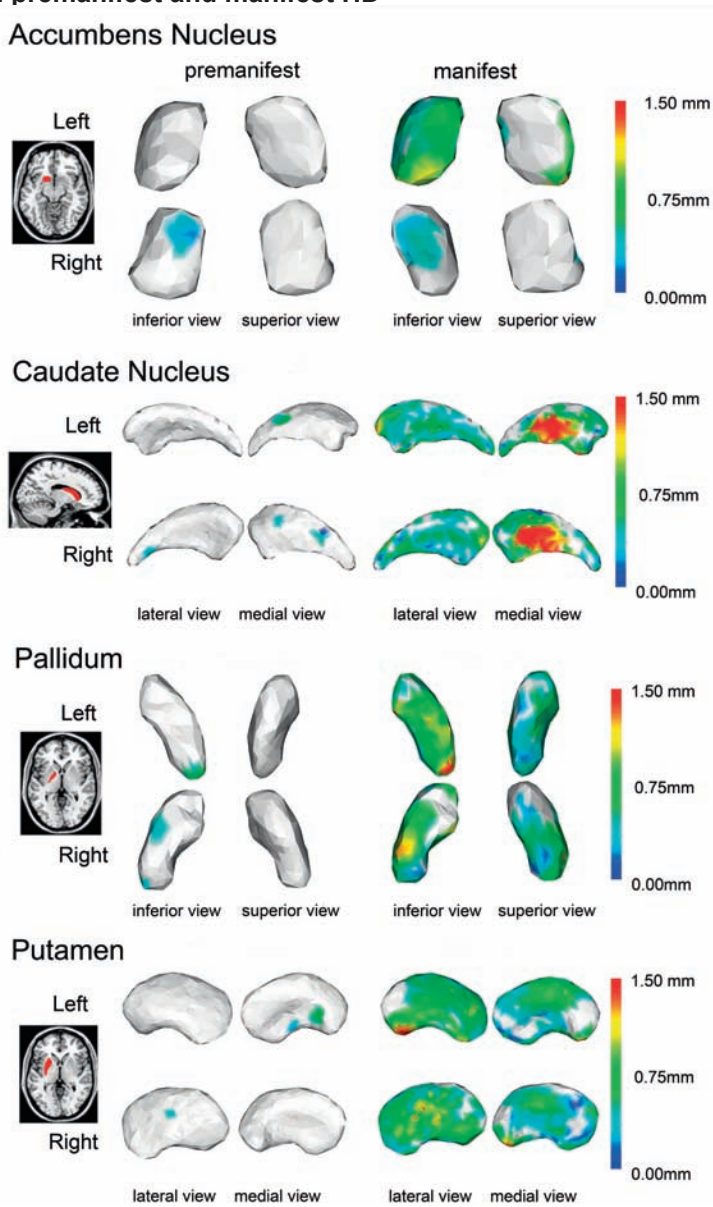

Figure 2: Shape analysis of accumbens nucleus, caudate nucleus, pallidum and putamen. On the left a T1-weighted image with one sided location of the structure analyzed. Group comparison of shape changes between the premanifest and control group on the second and third image. Left and right are separately displayed, and different views are provided. The fourth and fifth images display the control group versus the manifest HD group. The color bar on the right indicates the significant displacement in mm, white/gray indicates no significant displacement, while red indicates a displacement of 1,5 mm or higher

Shape analysis of amygdala, hippocampus and thalamus in premanifest and manifest HD

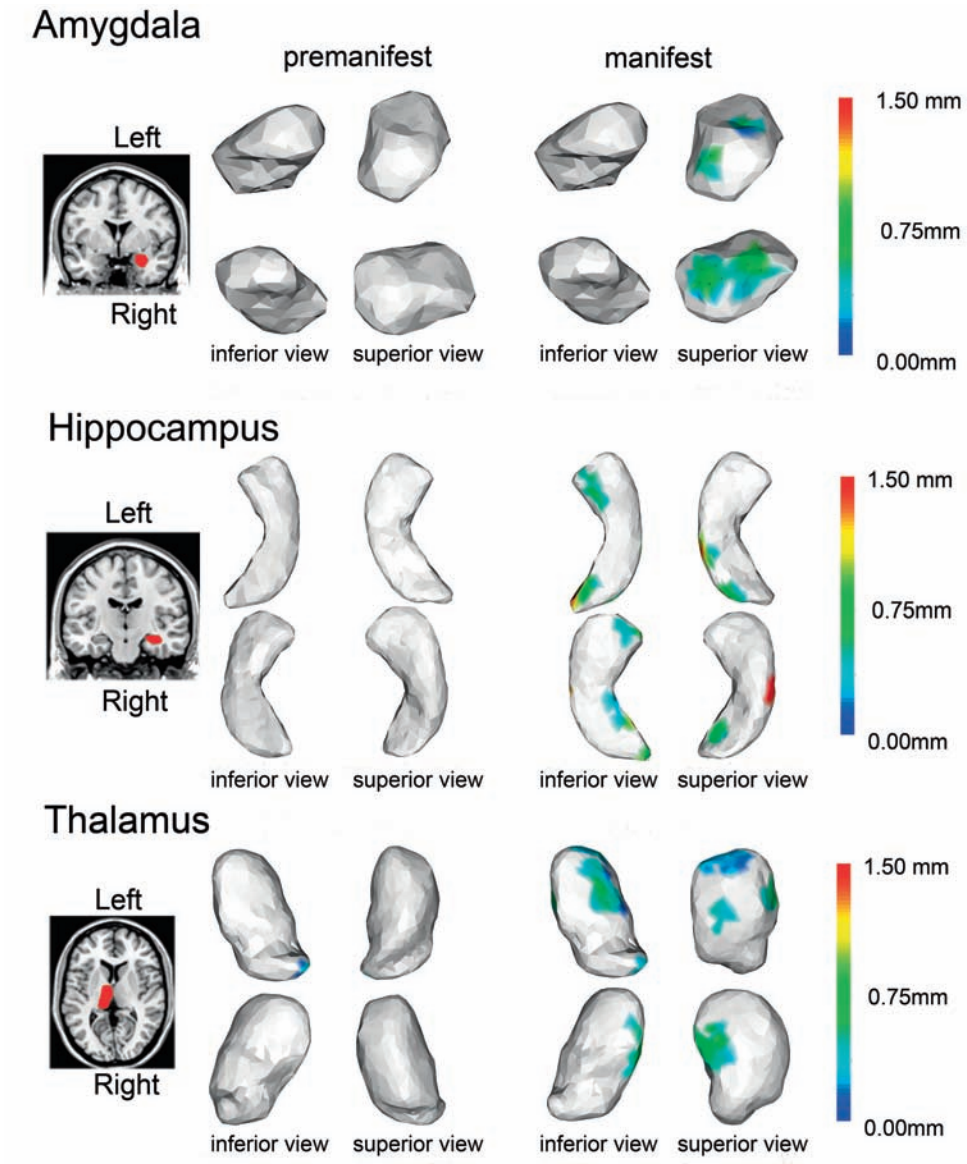

Figure 3: Shape analysis of amygdala, hippocampus and thalamus. On the left a T1-weighted image with one sided location of the structure analysed. Group comparison of shape changes between the premanifest and control group on the second and third image. Left and right are separately displayed, and different views are provided. The fourth and fifth images display the control group versus the manifest HD group. The colour bar on the right indicates the significant displacement in mm, white/gray indicates no significant displacement, while red indicates a displacement of 1,5 mm or higher

Shape analysis of accumbens nucleus, caudate nucleus, pallidum and putamen in the premanifest groups A and B

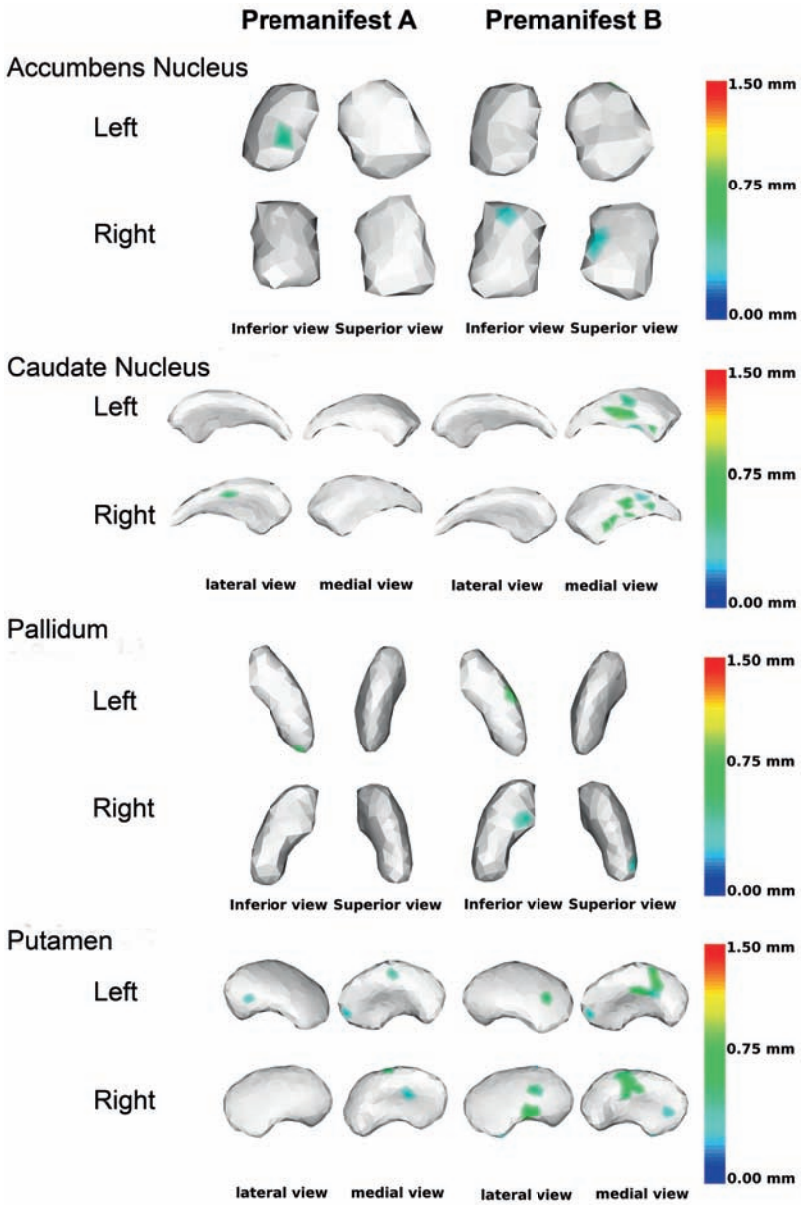

Figure 4: Shape analysis of accumbens nucleus, caudate nucleus, pallidum and putamen in the premanifest groups A and B.Group comparisons of shape changes between the premanifest far from expected onset (A) and close to expected onset (B) versus control group are shown. Left and right are separately displayed, and different views are provided. The colour bar on the right indicates the significant displacement in mm, white/gray indicates no significant displacement, while red indicates a displacement of 1,5 mm or higher

Shape analysis of amygdala, hippocampus and thalamus in the premanifest groups A and B

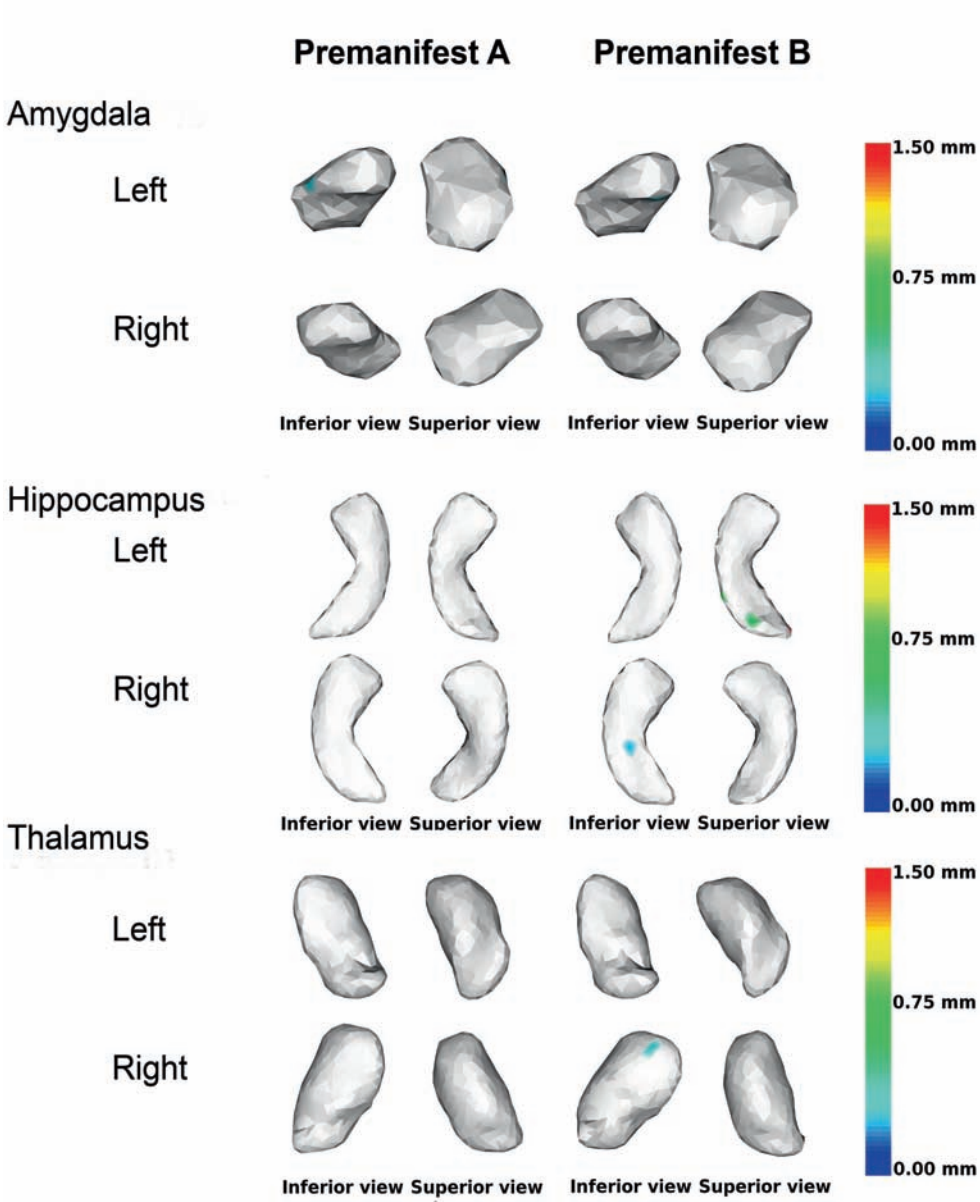

Figure 5: Shape analysis of amygdala, hippocampus and thalamus in the premanifest groups A and B. Group comparisons of shape changes between the premanifest far from expected onset (A) and close to expected onset (B) versus control group are shown. Left and right separately displayed, different views are provided. The color bar on the right indicates the significant displacement in mm, white/gray indicates no significant displacement, while red indicates a displacement of 1,5 mm or higher

The additional analysis within the premanifest group shows significant results in portions of the caudate nucleus, pallidum and putamen for the premanifest B group and hardly any significant results in premanifest A group (figures 4 and 5). In general this seems to point out more pronounced shape changes closer to disease onset.

Discussion

The main focus of this study was to investigate shape changes as a potentially sensitive measure to quantify pathologic changes in subcortical nuclei in HD, and in this way provide us with understanding of the atrophy patterns. The atrophy patterns acquired show localized changes in almost all structures in manifest HD, with a limited result in premanifest HD, most pronounced closer to predicted disease onset. Our analysis provides potential specific target areas for disease tracking measures, although longitudinal confirmation is needed.

Localized in vivo shape analysis is a relatively new analysis technique, not previously implemented in HD research. The potential scope for application of this analysis is evident as several studies demonstrated atrophy of the basal ganglia. Overall volume estimates may not capture the highly localized changes in these subcortical gray matter structures as these may not have a significant impact on overall volume. Shape analysis may bridge this gap. We emphasize that the shape analysis approach can be used in all stages of the disease, whereas microscopic studies can only be performed in the post-mortem stage. Post-mortem neuron counts imply that the parts where the most significant losses of neurons are seen in very advanced stages of HD, are also the areas where the shape or volume change would occur first. The pathologic studies available seem to point towards neuronal changes in specific portions of the caudate nucleus, namely the earliest changes are seen in the medial paraventricular portions of the caudate nucleus and in the tail of the caudate nucleus[5], which are also the areas seen in our shape analysis. According to Vonsattel *et al.* (1985) the neuropathological changes are seen along the antero-posterior, lateral-medial and ventro-dorsal axis. Also the dorsal part of the putamen, along the dorsal-ventral axis, has been reported to show the most significant neuronal loss[5;6], in our study the whole putamen seems affected and no specific conclusions on pattern can be drawn from this cross sectional analysis.

Our findings are in concurrence with the in vivo findings of Kassubek *et al*. (2005), who used a VBM approach describing regional striatal changes corresponding

to the dorso-ventral gradient of neuronal loss described in neuropathological studies[22]. Furthermore, regarding the thalamus, Kassubek *et al.* (2005) found thalamic subnuclei projecting to prefrontal areas (dorso-medial subnucleus) and connections to the striatum (ventromedian/parafascicular and ventrolateral nuclear complex) to display volume loss[23]. In our study the thalamus shows patchy displacements in predominantly ventral-medial and ventral-lateral areas. Although a VBM approach is methodologically very different from our approach, both give indications on local changes, and more importantly, the findings do seem to point to the same general areas.

The volume analysis in our cohort is in accordance with the literature[1;2;4;24]. Possibly, shape analysis is sensitive in detecting some changes that volumetric analysis could not pick up. The pallidum does show some regions being affected in the premanifest group, yet no significant result in overall volume difference could be detected. It must be noted that there is a decline in volume detectable when the left and right pallidum are combined and the premanifest group is split into two groups according to the predicted years to onset (data not shown). In contrast, in the premanifest group the accumbens nucleus, caudate nucleus and putamen show only minor regional shape changes, alongside their overall volume change, resulting in the conclusion that a more overall volume decrease is observed in these specific structures, rather than any specific regional change only. However, in manifest HD the shape differences provides specific knowledge about the location of the most significant neuron losses, and gives insight into the non-uniform pattern of atrophy of the subcortical gray matter structures. It might be that these specific areas could be targeted for sensitive assessment of pathological change, possibly correlating to disease onset. Perhaps the body of the caudate nucleus is in respect the most promising candidate as this is already demonstrated in the premanifest close to disease onset

As this regional shape analysis approach brings new insights as to where specifically these neurons are lost, it is possible to extend this in vivo knowledge to known anatomical regions within these structures. For example, the hippocampus anatomy is complex with multiple distinct functional substructures[25]. Neuropathologic reports on specific regions of the hippocampus being involved, such as the CA1 region in the R2/6 HD mouse model[26], could be supported by this type of in vivo analysis. This is also true for the thalamus, whose anatomy is known to be subdivided into several substructures. Our analysis shows the medial side to be affected, which could correspond to the mediodorsal part of the thalamus. Interestingly, Heinsen *et al.* (1999) reported that this part of the thalamus

is specifically affected in HD[27]. This part of the thalamus receives input from the prefrontal cortex and the limbic system and in turn relays them to the prefrontal association cortex. As a result, it plays a crucial role in cognitive functions such as attention, planning, organization, multi-tasking and memory which are known to be impaired in HD[28]. Haber *et al.*(2009) reviews all cortico-basal ganglia-thalamus circuits, and when correlating our findings to the described pathways one might argue that the regions found in our study correlate to the orbital frontal cortex and the anterior cingulate cortex (ventromedial striatum) and the (pre-) motor cortex (ventral anterior and ventral lateral nuclei) and to circuits between thalamus and basal ganglia in general as the mediodorsal part of the thalamus receives the bulk of the basal ganglia output[29].

More specific pathways on striatal-cortical connections are described by Lehericy *et al.*(2004)[30]. Extending this knowledge Draganski *et al.*(2008) demonstrated in healthy subjects in vivo the coexistence of clearly segregated and also overlapping connections from cortical sites to basal ganglia subregions[31]. They found that the the basal ganglia are connected in a rostrocaudal gradient of prefrontal connections in addition to projections to sensorimotor and parietal cortical areas. Using this knowledge we can extract from our own results the most severely affected subregions of the basal ganglia and their associated cortical projections. One example is the severe shape change in the body of the caudate nucleus which is, according to the connections described by Draganski *et al.*(2008), strongly connected to the dorsolateral prefrontal cortex[31]. This seems to be consistent with the above described thalamic connections of the prefrontal cortex which seem to be affected in HD. Another example is the dorsal part of the pallidum which has strong connections to the motor cortex, known to be affected in HD[1;31;32]. In this way the locally found shape changes in subcortical nuclei can be used to extend knowledge on affected pathways.

However, some caution must be taken not to over interpret these results, as the outer surface of a structure does not necessarily mean that neurons are lost within one small specific subnuclei, as the outer surface cannot give information about remodeling within one large structure or the specific neuronal cell changes, although it does give important clues as such.

A limitation of our study could be the usage of a relatively new software package from FSL for segmentation, which hasn't specifically been validated in HD. Visual inspection, however, did not reveal any significant mismatches. The method applied gives structure segmentation on an individual basis and can therefore be

used to compare groups. In contrast to this limitation clear several reasons exist in favor of using FIRST; first of all, compared to manual segmentation the automated segmentation uses voxel intensity in contrast to the sometimes difficult visual contrast differences, reducing a rater dependent bias. Secondly this automated technique is suitable for implantation on large datasets, whereas manual segmentation is labour intensive. Other techniques such as VBM, although proven to adequately compare groups, is prone to registration artifacts in the deep gray matter and may not be suitable for analysis of the pattern of atrophy in an individual subject[7;33].

Another limitation of this study is apparent in applying a statistical paradigm not specifically set for detecting changes in the premanifest group, where changes are relatively small. When less statistical scrutiny would be applied larger regions may show displacement, yet these standards were set before the analysis was performed and did not interfere with achieving the goal of the study, namely finding specific regional shape changes. Another limitation could also be the fact that our premanifest group is quite heterogeneous, in regards to the disease burden which has a substantial range. This disease burden score can be calculated by: (CAG repeat length – 35.5) x Age, and correlates well with striatal damage and expected age of onset[9]. This heterogeneity within the premanifest group has been addressed by performing an additional analysis within the premanifest group, showing the relationship of shape changes with disease onset. A final limitation is the cross sectional design, which is unsuited to prove the biomarker quality of localized shape changes and longitudinal follow up should be performed.
In conclusion, shape analysis provides new insights in patterns of atrophy in Huntington's disease. Specific parts of the subcortical gray matter structures are demonstrated to show major shape changes besides an overall volume change. This study assesses these differences in vivo and finds support in known pathologic findings in advanced HD. These localized areas provides not only additional knowledge in localized intrastructural atrophy patterns, but can also potentially serve as specific target areas for disease tracking.

Acknowledgment

The authors wish to thank the TRACK-HD study participants, the “CHDI/High Q Foundation”, a not-for-profit organization dedicated to finding treatments for HD, for providing financial support (www.chdifoundation.org), and all TRACK-HD investigators for their efforts in conducting this study (www.track-hd.net). We would like to thank BioRep for the CAG determinations. We would also like to acknowledge the following individuals personally for their contributions. Caroline Jurgens, Marie-Noelle Witjes-Ane and Ellen ‘t Hart for assistance with coordination and data collection, Gail Owen for coordination of data transfer and Felix Mudoh Tita for data monitoring.

References

1. Tabrizi SJ, Langbehn DR, Leavitt BR, et al. Biological and clinical manifestations of Huntington's disease in the longitudinal TRACK-HD study: cross-sectional analysis of baseline data. Lancet Neurol. 2009 Sep;8(9):791-801
2. Paulsen JS, Langbehn DR, Stout JC, et al. Detection of Huntington's disease decades before diagnosis: the Predict-HD study. J Neurol Neurosurg Psychiatry 2008;79:874-80
3. Bohanna I, Georgiou-Karistianis N, Hannan AJ, et al. Magnetic resonance imaging as an approach towards identifying neuropathological biomarkers for Huntington's disease. Brain Res Rev. 2008 Jun;58(1):209-25
4. Aylward EH. Change in MRI striatal volumes as a biomarker in preclinical Huntington's disease. Brain Res Bull 2007;72:152-58
5. Vonsattel JP, Myers RH, Stevens TJ, et al. Neuropathological classification of Huntington's disease. J Neuropathol Exp Neurol 1985;44:559-77
6. Roos RA, Pruyt JF, de Vries J, et al. Neuronal distribution in the putamen in Huntington's disease. J Neurol Neurosurg Psychiatry 1985;48:422-25
7. Bookstein FL. "Voxel-based morphometry" should not be used with imperfectly registered images. Neuroimage 2001;14(6):1454-62
8. Henley SM, Ridgway GR, Scahill RI, et al. Pitfalls in the use of voxel-based morphometry as a biomarker: examples from huntington disease. AJNR Am J Neuroradiol 2010;31:711-19
9. Penney JB, Jr., Vonsattel JP, MacDonald ME, et al. CAG repeat number governs the development rate of pathology in Huntington's disease. Ann Neurol 1997;41:689-92
10. Langbehn DR, Hayden MR, Paulsen JS. CAG-repeat length and the age of onset in Huntington disease (HD): A review and validation study of statistical approaches.Am J Med Genet B Neuropsychiatr Genet. 2010 Mar 5;153B(2):397-408.
11. Langbehn DR, Brinkman RR, Falush D, et al. A new model for prediction of the age of onset and penetrance for Huntington's disease based on CAG length. Clin Genet 2004;65:267-77
12. van den Bogaard SJ, Dumas EM, Acharya TP, et al. Early atrophy of pallidum and accumbens nucleus in Huntington's disease. J Neurol. 2011 Mar;258(3):412-20
13. Patenaude B, Smith S, Kennedy D, et al. FIRST - FMRIB's integrated registration and segmentation tool. 2007. In Human Brain Mapping Conference.
14. Patenaude B, Smith S, Kennedy D, et al. Improved Surface Models for FIRST. 2008. In Human Brian Mapping Conference.
15. Patenaude B. Bayesian Statistical Models of Shape and Appearance for Subcortical Brain Segmentation. 2007. Thesis. D.Phil.
16. de Jong LW, van der Hiele K, Veer IM, et al. Strongly reduced volumes of putamen and thalamus in Alzheimer's disease: an MRI study. Brain 2008;131(Pt 12):3277-85
17. Morey RA, Petty CM, Xu Y, et al. A comparison of automated segmentation and manual tracing for quantifying hippocampal and amygdala volumes. Neuroimage 2009;45(3):855-66
18. Morey RA, Selgrade ES, Wagner HR, et al. Scan-rescan reliability of subcortical brain volumes derived from automated segmentation. Hum Brain Mapp 2010;31(11):1751-62
19. Ferrarini L, Olofsen H, Palm WM, et al. GAMEs: growing and adaptive meshes for fully automatic shape modeling and analysis. Med Image Anal 2007;11:302-14
20. Ferrarini L, Palm WM, Olofsen H, et al. MMSE scores correlate with local ventricular enlargement in the spectrum from cognitively normal to Alzheimer disease. Neuroimage 2008;39:1832-38
21. Ferrarini L, Palm WM, Olofsen H, et al. Ventricular shape biomarkers for Alzheimer's disease in clinical MR images. Magn Reson Med 2008;59:260-67
22. Kassubek J, Juengling FD, Kioschies T, et al. Topography of cerebral atrophy in early Huntington's disease: a voxel based morphometric MRI study. J Neurol Neurosurg Psychiatry 2004;75:213-20
23. Kassubek J, Juengling FD, Ecker D, et al. Thalamic atrophy in Huntington's disease co-varies with

cognitive performance: a morphometric MRI analysis. Cereb Cortex 2005;15:846-53
24. Rosas HD, Koroshetz WJ, Chen YI, et al. Evidence for more widespread cerebral pathology in early HD: an MRI-based morphometric analysis. Neurology 2003;60:1615-20
25. van Strien NM, Cappaert NL, Witter MP. The anatomy of memory: an interactive overview of the parahippocampal-hippocampal network. Nat Rev Neurosci 2009;10:272-82
26. Murphy KP, Carter RJ, Lione LA, et al. Abnormal synaptic plasticity and impaired spatial cognition in mice transgenic for exon 1 of the human Huntington's disease mutation. J Neurosci 2000;20:5115-23
27. Heinsen H, Rub U, Bauer M, et al. Nerve cell loss in the thalamic mediodorsal nucleus in Huntington's disease. Acta Neuropathol 1999;97(6):613-22
28. Lemiere J, Decruyenaere M, Evers-Kiebooms G, et al. Cognitive changes in patients with Huntington's disease (HD) and asymptomatic carriers of the HD mutation--a longitudinal follow-up study. J Neurol 2004;251(8):935-42
29. Haber SN, Calzavara R. The cortico-basal ganglia integrative network: the role of the thalamus. Brain Res Bull 2009;78(2-3):69-74
30. Lehericy S, Ducros M, Van de Moortele PF, et al. Diffusion tensor fiber tracking shows distinct corticostriatal circuits in humans. Ann Neurol 2004;55(4):522-29
31. Draganski B, Kherif F, Kloppel S, et al. Evidence for segregated and integrative connectivity patterns in the human Basal Ganglia. J Neurosci 2008;28(28):7143-52
32. Dumas EM, van den Bogaard SJ, Ruber ME, et al. Early changes in white matter pathways of the sensorimotor cortex in premanifest Huntington's disease. Hum Brain Mapp. 2012 Jan;33(1):203-12.
33. Frisoni GB, Whitwell JL. How fast will it go, doc? New tools for an old question from patients with Alzheimer disease. Neurology 2008;70(23):2194-95